WS_2 2D Nanosheets in 3D Nanoflowers

Arunvinay Prabakaran, *[a] Frank Dillon,[a] Jodie Melbourne, [a] Lewys Jones, [a] Rebecca J Nicholls, [a] Jude Britton, [a] Antal A Koos, [a] Peter Nellist, [a] Nicole Grobert [a]

Received (in XXX, XXX) Xth XXXXXXXXX 20XX, Accepted Xth XXXXXXXXX 20XX

DOI: 10.1039/b000000x

In this work it has been established that 3D nanoflowers of WS_2 synthesized by chemical vapour deposition are composed of few layer WS_2 along the edges of the petals. An experimental study to understand the evolution of these nanostructures shows the nucleation and growth along with the compositional changes they undergo.

The structural analogy of transition metal dichalcogenides[1] to graphite's layered structure, held together by van der Waals forces, prompted the synthesis and characterisation of inorganic fullerene-like structures (IF)[2] and inorganic nanotubes (IN) of WS_2[3] in 1992[4] and MoS_2 in 1995.[5] The IF and IN structures resemble fullerenes and carbon nanotubes respectively[6]. They possess interesting mechanical[7] and electronic properties[8] which find applications in high temperature solid state lubricants and catalysis.[9] Commercial quantities of these structures are synthesised from oxide template which limit the morphology and enhance control[6]. However, since the discovery of graphene in 2004[10], two dimensional material systems have been in demand. Consequently the field is now actively pursuing inorganic graphene analogues (IGA)[11], which due to their inherent band gap, are potential components in creating 2D heterostructures.[12] However, still a reliable method to synthesize large quantities of this material form hasn't been established. Nanosheets of IGA possess excellent electronic[14] and optical properties[15] which find applications in field effect transistors[16] and photodetectors[17] respectively. WS_2 nanomaterials, in particular have shown potential applications as industrial catalysts in denitrogenation and hydrodesulphurization processes[18,19], high performance nanocomposites[20], and lithium batteries.[21] Nevertheless, to exploit the properties of WS_2 nanomaterials, methods that enable precise control of the morphology are required.

In this work, a fast, catalyst free and easily scalable chemical vapour deposition (CVD) technique for the controlled synthesis of well-defined tungsten disulphide (WS_2) nanomaterials on (100) silicon-based substrates using tungsten(VI)chloride (WCl_6-2 mmol at 99.9% purity) and sulphur (20 mmol at 80% purity) as precursors is presented in Fig S1. The predominant morphology (>90%) obtained by this process is WS_2 nanoflower confirmed using electron microscopy as shown in Fig.1a and the chemistry verified using XRD and Raman in Fig S2. The morphology of the WS_2 nanostructures synthesised by the CVD technique can be tailored through the variation of just two key parameters: time and temperature. Though a similar strategy has been employed previously to obtain nanostructures of WS_2 and MoS_2[22], herein the process has been greatly simplified by using shorter time periods to enhance control and scalability.

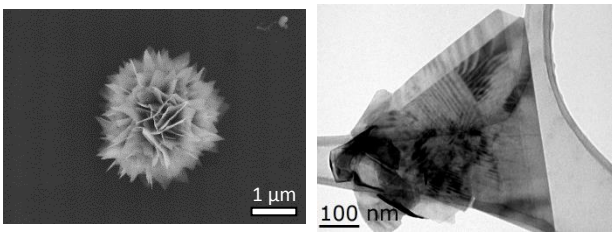

Figure 1.a) SEM image of 3D Nanoflower b) TEM images of a petal (flake)/2D nanosheet from a 3D nanoflower

WS_2 nanoflowers are composed of petals that resemble an equilateral triangular as shown in Fig 1b. Few layer edges with atomic resolution has been observed on analysis using a double aberration corrected JOEL 2200 MCO operated at 200kV in STEM mode and high angle annular dark field (HAADF) detector. Though nanoflowers were reported in 2004[22], as yet, a detailed analysis of their structure has not been undertaken. This study looks to comprehend the structure of the nanoflower by disassembling it with the help of sonication. The nanoflowers disassembled into triangular petals (flakes) on sonication with one corner always broken, which suggests that these triangles are connected at only one of the edges to form the assembly of 3D nanoflowers. We observed 10-100's of these triangular petals combining together to form spherical nanoflower structures as suggested by Li *et al.*[22] and evident from the SEM micrograph in Fig 1a.

The nanoflowers are made up of molecular sheets stacked together with a lattice spacing of 3.1 Å and lattice fringes of 0.62 nm, inferred for WS_2. In Fig 2a, a cluster of the petals which constitute the nanoflowers is visualised from the edge view (beam perpendicular to c-axis), to reveal 6-8 molecular layers of WS_2. These WS_2 were stacked on top of each other to form the petals. The distribution of the number of molecular layers to form the petal is not very uniform and varies from few layer (2-4) to increased number of layers up to 12/14. With the beam parallel to the c axis, the hexagonal packing can be clearly observed at the edges where the number of layers have reduced considerably to

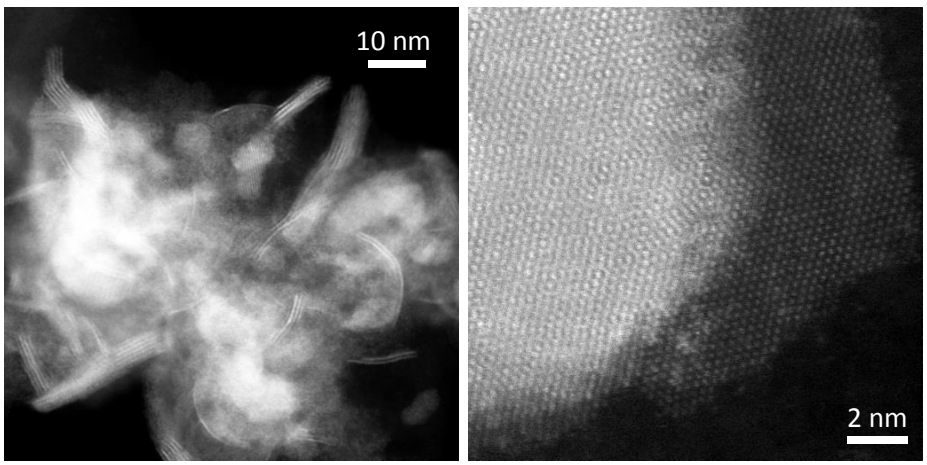

Figure 2. STEM image depicting a) stacking of atomic layers in petal; b) atomic layers in WS_2 flake

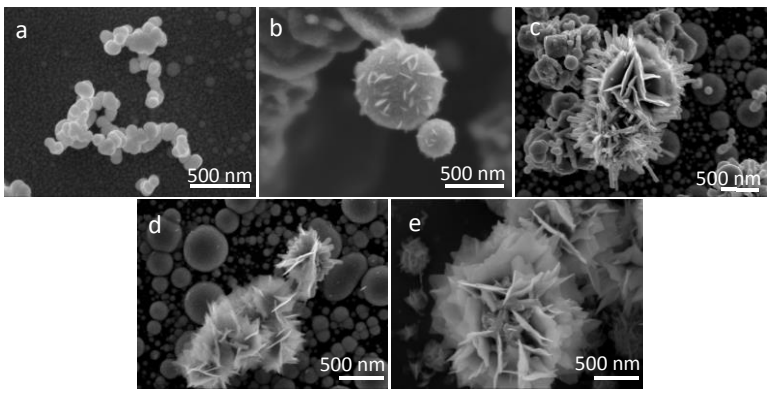

Figure 3.Evolution of nanoflower structure with progress in time periods from 10s to 1800s at 850ºC

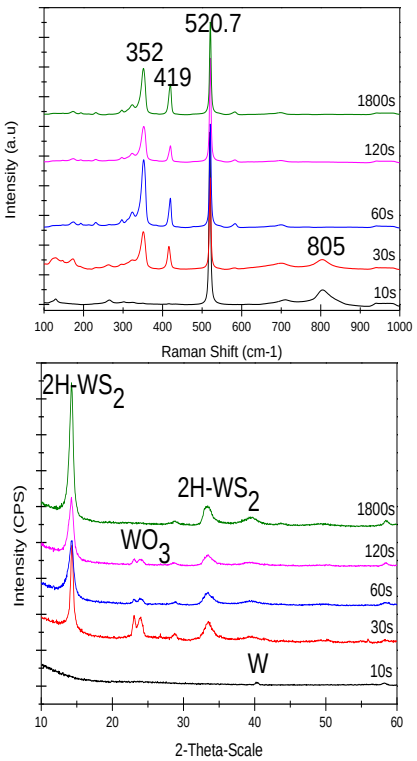

Figure 4. a) Raman spectroscopy b) XRD of deposits for various time periods from 10s to 1800s at 850ºC

reveal mono- and bi-layer regions. This is a significant observation since it highlights that the nanoflowers are composed of few layer nanosheets at the edges. These few layer (mono- and bi-layer) edges are visible in the Fig 2b. As we move towards the centre of the petal the layers stack up progressively forming Moiré fringes which are visible near the centre of the petal.

In order to understand the evolution of these structures, short time nucleation experiments were carried out. The process parameters were similar to the CVD experiments employed to produce nanoflowers. However, the nucleation experiments were performed at very short time periods ranging from 10 s, 30 s, 60 s, and 120 s to 1800 s. The different stages of nucleation of the nanoflower are shown in Fig 3 and clearly shows the evolution process involved in forming these nanostructures. This different stages of evolution has also been studied using XRD and Raman spectroscopy and the results are shown in Fig. 4a and 4b respectively. Initially, nanoparticles of tungsten are formed, as confirmed by XRD at 10 s in Fig 4b. These particles are usually agglomerated as seen in Fig 3a. Oxidation of these nanoparticles over time was observed with the aid of EDX as presented in Fig S3. As reaction time was increased to 30 s, intermediate phases of tungsten- oxide and sulphide were observed as evident from the WO_3 and WS_2 peaks in XRD. This could be sulphur progressively reacting with the oxide nanoparticles, as proposed by Tenne *et al.*[22], forming flake like structures on the surface, visible in Fig. 3b. The oxides may be formed when particles are oxidised when exposed to the atmosphere while transferring them for characterisation. The morphology after 60 s in Fig.3c shows the formation of petals from these particles and also the presence of tubular structures. With time, the tubular morphology disappears and only flakes are observed as in Fig 3d. Over longer time periods of 1800 s all of the tubular structures observed in Fig 3c & 3d are converted to flakes and flowers with predominantly large flakes/ petals as observed from Fig.3e and they exhibit characteristic WS_2 signals in Raman and XRD.

The synthesis process observed in this work seems to follow a combination of the mechanisms described previously in literature. W species are formed in the first 10 s, which are transformed into intermediate species of WO_xS_y over 120 s, which eventually form a pure WS_2 phase after 300 s (5 min). This is determined by XRD, which clearly shows the suppression of oxide phases and dominance of sulfide phase with the increase in time from 10 s to 1800 s. Raman spectroscopy also shows the characteristic A_1g (352 cm^{-1}) and E_2g (420 cm^{-1}) belonging to

WS_2 phase which feature in the later stages of the process. Thus the initial phase of the experiment shows the presence of an oxide phase in both XRD and Raman. The source of this oxygen is uncertain and is difficult to trace.

Tenne *et al.*[23] highlights a similar mechanism for the formation of IF-WS_2 nanoparticles using WCl_n and H_2S precursors. A major difference from that work is the formation of WS_2 nanosheets on the surface of the nanoparticle in random directions leading to nanoflower formation in contrast to confined growth in IF-WS_2. It is reported that the WCl_n on heating first forms W species, possibly WCl_xS_y, which on subsequent reaction leads to the formation of a pure WS_2 phase. Another mechanism proposed based on TEM-EDS, was amorphous WS_3 formation enhancing IF-WS2 formation through sulphur abstraction and crystallization[22]. Li *et al.*[22] reported the use of sulphur both as a reductant and sulphurisation agent at the same time. They reported a self-redox and metathesis reaction, resulting in a stepwise sulphurisation of $MoCl_5$ to form MoS_xCl_y intermediate at low temperatures of 515 ^oC and pure MoS_2 phase at 800 ^oC. This same mechanism is likely to hold for WS_2.

The potential use of nanoflowers as a precursor/source for nanosheets would make it an attractive process for 2D material as large amounts (grams) of these nanoflowers can be produced by a relatively simple CVD process. Furthermore, these nanoflowers could be studied for applications such as catalysts for hydrogen evolution due to the presence of few layer edges.

Conclusions

In summary, we have reported the presence of 2D nanosheets in 3D nanoflowers of WS_2 nanomaterials. Using aberration corrected transmission electron microscopy, we observed the presence of few layer WS_2 at the edges of these 2D nanosheets/petals and also the progressive stacking of these layers to form the petals that in turn give the 3D nanoflower morphology. This study eludes to the possibility of using 3D nanoflowers, which are relatively easy to synthesize using a simple scalable atmospheric chemical vapour deposition method, as precursors for 2D nanosheets. In addition, the process of nucleation has been followed closely to reveal the role of oxide nanoparticles in the formation of these nanostructures.

Acknowledgment:. NanoTp, ERC starting grant

Notes and references

[a] *Department of Materials, University of Oxford, Parks Road, OX1 3PH, UK. E-mail:* nicole.grobert@materials.ox.ac.uk

1. J. A Wilson and A D. Yoffe, *Adv. Phys.*, 1969, **18**, 193–335.
2. Y. Feldman, G. L. Frey, M. Homyonfer, V. Lyakhovitskaya, L. Margulis, H. Cohen, G. Hodes, J. L. Hutchison, and R. Tenne, 1996, **2**, 5362–5367.
3. A. Rothschild, J. Sloan, and R. Tenne, 2000, 5169–5179.
4. G. Tenne, R. Margulis, L. Genut, M. & Hodes, *Nature*, 1992, **360**, 444–446.
5. Y. Feldman, E. Wasserman, D. J. Srolovitz, and R. Tenne, *Science*, 1995, **267**, 222–5.
6. R. Tenne, *Nat. Nanotechnol.*, 2006, **1**, 103–111.
7. Y. Q. Zhu, T. Sekine, Y. H. Li, M. W. Fay, Y. M. Zhao, C. H. Patrick Poa, W. X. Wang, M. J. Roe, P. D. Brown, N. Fleischer, and R. Tenne, *J. Am. Chem. Soc.*, 2005, **127**, 16263–72.
8. G. Seifert, H. Terrones, M. Terrones, G. Jungnickel, and T. Frauenheim, *Phys. Rev. Lett.*, 2000, **85**, 146–9.
9. R. R. Chianelli, M. H. Siadati, M. P. De la Rosa, G. Berhault, J. P. Wilcoxon, R. Bearden, and B. L. Abrams, *Catal. Rev.*, 2006, **48**, 1–41.
10. K. S. Novoselov, a K. Geim, S. V Morozov, D. Jiang, Y. Zhang, S. V Dubonos, I. V Grigorieva, and a a Firsov, *Science*, 2004, **306**, 666–9.
11. S. Z. Butler, S. M. Hollen, L. Cao, Y. Cui, J. A. Gupta, H. R. Gutie, T. F. Heinz, S. S. Hong, J. Huang, A. F. Ismach, E. Johnston-halperin, M. Kuno, V. V Plashnitsa, R. D. Robinson, R. S. Ruoff, S. Salahuddin, J. Shan, L. Shi, O. M. G. Spencer, M. Terrones, W. Windl, and J. E. Goldberger, 2013.
12. A. K. Geim and I. V Grigorieva, *Nature*, 2013, **499**, 419–25.
13. H.Terrones, F. Lopez-Urias and M.Terrnoes, *Nature Scientific reports*, 2013, **3**, 1549
14. Z. Zeng, Z. Yin, X. Huang, H. Li, Q. He, G. Lu, F. Boey, and H. Zhang, *Angew. Chem. Int. Ed. Engl.*, 2011, **50**, 11093–7.
15. A. Splendiani, L. Sun, Y. Zhang, T. Li, J. Kim, C.-Y. Chim, G. Galli, and F. Wang, *Nano Lett.*, 2010, **10**, 1271–5.
16. B. Radisavljevic, a Radenovic, J. Brivio, V. Giacometti, and a Kis, *Nat. Nanotechnol.*, 2011, **6**, 147–50.
17. W. Shi and C. Run-feng, 2013, **29**, 667–677.
18. A. Sobczynski, A. Yildiz, A. J. Bard, A. Campion, M. A. Fox, T. Mallouk, S. E. Webber, and J. M. White, 1988, 2311–2315.
19. P. Luque, E. Medina, and A. Olivas, 2012, **2**, 569–574.
20. L. Rapoport, N. Fleischer, and R. Tenne, *J. Mater. Chem.*, 2005, **15**, 1782.
21. G. X. Wang, S. Bewlay, J. Yao, H. K. Liu, and S. X. Dou, *Electrochem. Solid-State Lett.*, 2004, **7**, A321.
22. X.-L. Li, J.-P. Ge, and Y.-D. Li, *Chemistry*, 2004, **10**, 6163–71.
23. A. Margolin, F. L. Deepak, R. Popovitz-Biro, M. Bar-Sadan, Y. Feldman, and R. Tenne, *Nanotechnology*, 2008, **19**, 095601.